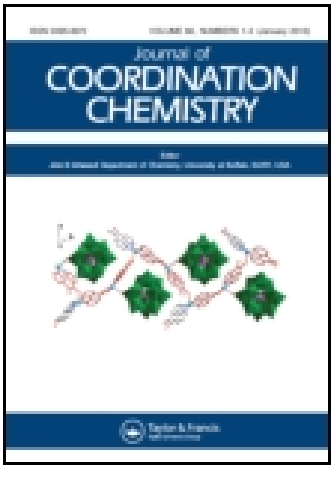

Journal of Coordination Chemistry
Publication details, including instructions for authors and subscription information:
http://www.tandfonline.com/loi/gcoo20

Synthesis, crystal structure, antioxidation and DNA-binding properties of a dinuclear copper(II) complex with bis(N-salicylidene)-3-oxapentane-1,5-diamine

Huilu Wu[a], Yuchen Bai[a], Yanhui Zhang[a], Zhen Li[a], Mingchang Wu[a], Chengyong Chen[a] & Jiawen Zhang[a]

[a] School of Chemical and Biological Engineering, Lanzhou Jiaotong University, Lanzhou, PR China

Accepted author version posted online: 28 Aug 2014.Published online: 23 Sep 2014.

To cite this article: Huilu Wu, Yuchen Bai, Yanhui Zhang, Zhen Li, Mingchang Wu, Chengyong Chen & Jiawen Zhang (2014) Synthesis, crystal structure, antioxidation and DNA-binding properties of a dinuclear copper(II) complex with bis(N-salicylidene)-3-oxapentane-1,5-diamine, Journal of Coordination Chemistry, 67:18, 3054-3066, DOI: 10.1080/00958972.2014.959507

To link to this article: http://dx.doi.org/10.1080/00958972.2014.959507

Journal of Coordination Chemistry, 2014
Vol. 67, No. 18, 3054–3066, http://dx.doi.org/10.1080/00958972.2014.959507

Synthesis, crystal structure, antioxidation and DNA-binding properties of a dinuclear copper(II) complex with bis(*N*-salicylidene)-3-oxapentane-1,5-diamine

HUILU WU*, YUCHEN BAI, YANHUI ZHANG, ZHEN LI, MINGCHANG WU, CHENGYONG CHEN and JIAWEN ZHANG

School of Chemical and Biological Engineering, Lanzhou Jiaotong University, Lanzhou, PR China

(*Received 18 April 2014; accepted 24 July 2014*)

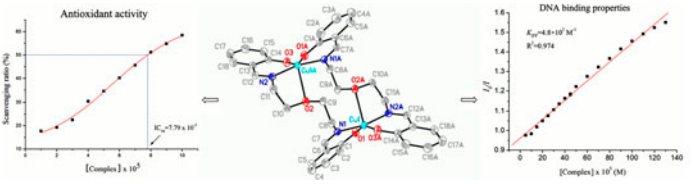

A Schiff base bis(*N*-salicylidene)-3-oxapentane-1,5-diamine (H_2L) and its Cu(II) complex, $[Cu_2(L)_2]\cdot CHCl_3$, have been synthesized and characterized by physicochemical and spectroscopic methods. Single-crystal X-ray analysis revealed that the complex is a centrosymmetric binuclear neutral entity, in which Cu(II) is a five-coordinate in a distorted trigonal bipyramidal geometry. The DNA-binding properties of the free ligand and the complex have been investigated by electronic absorption, fluorescence, and viscosity measurements. The results suggest that the H_2L and the complex to DNA *via* the intercalation mode and the binding affinity of the complex were higher than that of the H_2L. The intrinsic binding constants K_b of the ligand and the complex are 2.2×10^4 and 2.7×10^4 M^{-1}, respectively. Antioxidant assay *in vitro* shows the Cu(II) complex possesses significant antioxidant activities and better scavenging activity than the H_2L and other antioxidants.

Keywords: Bis(*N*-salicylidene)-3-oxapentane-1,5-diamine; Copper(II) complex; Crystal structure; DNA-binding; Antioxidant

1. Introduction

Schiff bases are an important class of compounds in medicinal and pharmaceutical fields. They show biological applications including antibacterial, antifungal [1–5], and antitumor activities [6, 7]. Metal–organic complexes offer the possibility of new functional materials, in which pore size, coordination forms, and functionality could be varied [8]. Diamino

*Corresponding author. Email: wuhl@mail.lzjtu.cn

Schiff bases and their complexes have been used as biological models to understand the structures of biomolecules and biological processes [9, 10].

The syntheses and interactions of transition metal complexes with DNA and protein have been an active field of research. Interest in this area is aimed at gaining insight into the mechanism involving site-specific recognition of DNA, the biochemical procedures governing protein sequencing, foot-printing and folding studies, understanding the reactive models for protein–nucleic acid interactions, application of probes of DNA structure, and obtaining information about the rational design and synthesis of new types of pharmaceutical molecules. To search for new restriction enzymes and anticancer therapeutic agents, much effort has been made in synthesis and property investigation of mimics. These complexes can bind to DNA in many non-covalent modes, such as ionic bonds, hydrogen bonds, $\pi \rightarrow \pi^*$ interactions, and hydrophobic interactions [11, 12]. The interactions of small inorganic–organic molecules with DNA have attracted attention because of their interference with important events in cells of living organisms [13–16].

DNA binding is the critical step for DNA activity. To design effective chemotherapeutic agents and better anticancer drugs, it is essential to explore the interactions of metal complexes with DNA [17, 18]. An understanding of how these small molecules bind to DNA will be potentially useful in the design of new drugs, significantly sensitive spectroscopic or diagnostic probes and reactive agents, which can recognize specific sites or conformations of DNA [19–22]. In recent years, inorganic–organic metal complexes such as Schiff base derivatives and their transition metal complexes have been investigated in interactions between complexes and DNA. Antioxidant activities of the complex were determined by hydroxyl radical (OH•) scavenging methods *in vitro* [23, 24].

In this study, a Cu(II) complex of bis(*N*-salicylidene)-3-oxapentane-1,5-diamine was synthesized and its interaction with DNA was studied via electronic absorption spectroscopy, viscosity, and fluorescence spectroscopy. In addition, the antioxidant activities of the complex were determined by hydroxyl radical (HO•) scavenging methods *in vitro*.

2. Experimental

2.1. *Measurements and methods*

C, H, and N elemental analyses were determined using a Carlo Erba 1106 elemental analyzer. IR spectra were recorded from 4000 to 400 cm^{-1} with a Nicolet FT-VERTEX 70 spectrometer using KBr pellets. The fluorescence spectra were recorded on a LS-45 spectrofluorophotometer. Electronic spectra were taken on a Lab-Tech UV Bluestar spectrophotometer. Antioxidant activities containing the hydroxyl radical (OH•) were performed in a water bath with a 722sp spectrophotometer.

All chemicals were of analytical grade. Calf thymus DNA (CT-DNA), ethidium bromide (EB), nitroblue tetrazolium nitrate, methionine, and riboflavin were obtained from Sigma-Aldrich Co. (USA) and used without purification. Tris–HCl buffer and EDTA-Fe(II) solution were prepared using bidistilled water. The stock solution of complex was dissolved in DMF at 3×10^{-3} M L^{-1}. All chemicals used were of analytical grade. The experiments involving interaction of the ligand and the complex with CT-DNA were carried out in double distilled water buffer containing 5 mM Tris and 50 mM NaCl and adjusted to pH 7.2 with hydrochloric acid.

2.2. *Preparation of 3-oxapentane-1,5-diamine*

3-Oxapentane-1,5-diamine was synthesized following the procedure [25]. $-C_4H_{12}N_2O$ (104.1): (Found (%): C, 45.98; H, 11.50; N, 26.76. Calcd (%): C, 46.13; H, 11.61; N, 26.90). Selected IR data: (KBr ν (cm^{-1})), 1120 (ν_{C-O-C}), 3340 (ν_{-NH2}).

2.3. *Preparation of bis(N-salicylidene)-3-oxapentane-1,5-diamine (H_2L)*

For the synthesis of H_2L, salicylaldehyde (10 mM, 1.22 g) in EtOH (5 mL) was added dropwise to a 5 mL EtOH solution of 3-oxapentane-1,5-diamine (10 mM, 1.04 g). After completion of addition, the solution was stirred for an additional 4 h at 78 °C. After cooling to room temperature, the precipitate was filtered. The product was dried in vacuo, giving a yellow crystalline solid. The synthetic route for H_2L is shown in scheme 1. Yield: 1.65 g (73.0%). $-C_{18}H_{20}O_3N_2$ (312.4): (Found (%): C, 69.30; H, 6.51; N, 8.89. Calcd (%): C, 69.21; H, 6.45; N, 8.97). Selected IR data: (KBr ν (cm^{-1})), 1637($\nu_{C=N}$), 1286(ν_{C-O-C}), 3458 (ν_{OH}), stretching frequency, respectively. UV–vis (DMF): λ = 275, 311 nm.

2.4. *Preparation of $[Cu_2(L)_2]\cdot CHCl_3$*

To a stirred solution of H_2L (0.312 g, 1 mM) in MeOH (5 mL) was added $Cu(NO_3)_2(H_2O)_3$ (0.241 g, 1 mM) in MeOH (5 mL). The blue sediment generated rapidly. The precipitate was filtered off, washed with MeOH and absolute Et_2O, and dried in vacuo. The dried precipitate was dissolved in $CHCl_3$ to form a blue solution. Blue block crystals of $[Cu_2(L)_2]\cdot CHCl_3$ suitable for X-ray diffraction studies were obtained by evaporation of the $CHCl_3$ for a few weeks at room temperature. Yield: 0.218 g (41.4%). $-Cu_2C_{38}H_{38}Cl_6N_4O_6$ (986.50): (Found (%): C, 57.55; H, 4.88; N, 7.38. Calcd (%): C, 57.82; H, 4.85; N, 7.49). Selected IR data: (KBr ν (cm^{-1})), 1147 (ν_{C-O-C}), 1627 ($\nu_{C=N}$) stretching frequency, respectively. UV–vis (DMF): λ = 294, 370 nm.

2.5. *X-ray structure determination of $[Cu_2(L)_2]\cdot CHCl_3$*

A suitable single crystal was mounted on a glass fiber, and the intensity data were collected on a Bruker Smart CCD diffractometer with graphite-monochromated Mo Kα radiation (λ = 0.71073 Å) at 296 K. Data reduction and cell refinement were performed using

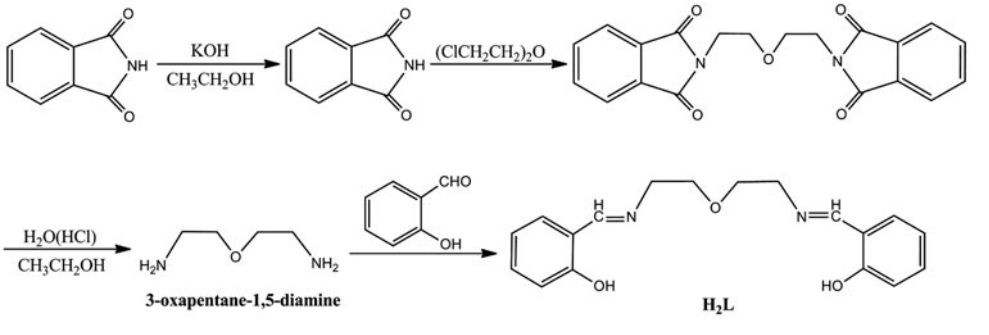

Scheme 1. Synthetic route for H_2L.

Table 1. Crystallographic data and data collection parameters for $[Cu_2(L)_2]\cdot CHCl_3$.

Formula	$Cu_2C_{38}H_{38}Cl_6N_4O_6$
Molecular weight (g m^{-1})	986.50
Crystal system	Monoclinic
Space group	*P2(1)/c*
Unit cell dimensions	
a (Å)	13.1746(4)
b (Å)	16.6027(5)
c (Å)	9.4906(3)
α (°)	90
β (°)	102.3060(10)
γ (°)	90
Volume (Å^3)	2028.22(11)
Z	2
T (K)	296(2)
D (calculated) (g cm^{-3})	1.615
Absorption coefficient (mm^{-1})	1.495
F (0 0 0)	1004
Crystal size (mm)	0.38 × 0.30 × 0.28
θ Range for data collection (°)	2.10–25.00
Reflections collected	19,536
Independent reflections	4648 [*R*(int) = 0.0334]
Index ranges	$-17 \le h \le 17$, $-21 \le k \le 20$, $-12 \le l \le 12$
Refinement method	Full-matrix least-squares on F^2
Data/restraints/parameters	4648/0/254
Goodness-of-fit on F^2	1.068
Finial R_1 and wR_2 [$I > 2\sigma(I)$]	$R_1 = 0.0330$, $wR_2 = 0.0824$
R indices (all data)	$R_1 = 0.0385$, $wR_2 = 0.0941$
Largest difference in peak and hole (e Å^{-3})	0.713 and −0.705

SMART and SAINT programs. Data reduction and cell refinement were performed using SAINT programs [26]. The absorption corrections were carried out by the empirical method. The structure was solved by direct methods and refined by full-matrix least-squares against F^2 using SHELXTL software [27].

All hydrogens were found in different electron maps and were subsequently refined in a riding-model approximation with C–H distances from 0.93 to 0.97 Å and $U_{iso}(H) = 1.2\ U_{eq}(C)$ or $U_{iso}(H) = 1.5\ U_{eq}(C)$. A summary of parameters for the data collections and refinements are given in table 1.

2.6. *DNA binding experiments*

Metal complexes can bind to DNA according to three possible patterns: (1) electrostatic interaction, in which the metal complexes are electrostatically adsorbed on the phosphates of DNA, (2) intercalative binding, in which the metal complexes intercalate into the base pairs of the double-stranded DNA, and (3) groove binding, in which the metal complexes interact with the grooves of DNA [28]. Absorption titration experiments were performed with fixed concentrations of the compounds, while gradually increasing the concentration of CT-DNA. The required amount of CT-DNA was added to both the compound solution and the reference solution to eliminate the absorbance of CT-DNA itself. From the absorption titration data, the binding constant (K_b) was determined using the equation [29]:

$$[\mathrm{DNA}]/(\varepsilon_a - \varepsilon_f) = [\mathrm{DNA}]/(\varepsilon_b - \varepsilon_f) + 1/K_b(\varepsilon_b - \varepsilon_f)$$

where [DNA] is the concentration of CT-DNA in the base pairs, ε_a corresponds to the observed extinction coefficient (A_{obsd}/[M]), ε_f corresponds to the extinction coefficient of the free compound, ε_b is the extinction coefficient of the compound when fully bound to CT-DNA, and K_b is the intrinsic binding constant. The ratio of slope to intercept in the plot of [DNA]/($\varepsilon_a - \varepsilon_f$) *versus* [DNA] gave the value of K_b.

The fluorescence of EB intercalated into DNA can be quenched by the addition of a second molecule [30, 31]. The extent of the fluorescence quenching of EB bound to CT-DNA can be used to determine the extent of binding between the second molecule and CT-DNA. The competitive binding experiments were carried out in the buffer by keeping [DNA]/[EB] = 1.13 and varying the concentrations of the compounds. The fluorescence spectra of EB were measured using an excitation wavelength of 520 nm, and the emission range was set between 550 and 750 nm. The spectra were analyzed according to the classical Stern–Volmer equation [32]: $I_0/I = 1 + K_{sv}[Q]$, where I_0 and I are the fluorescence intensities at 599 nm in the absence and presence of the quencher, respectively, K_{sv} is the linear Stern–Volmer quenching constant, and [Q] is the concentration of the quencher. In these experiments, [CT-DNA] = 2.5×10^{-3} M/L, [EB] = 2.2×10^{-3} M/L.

Viscosity measurements were carried out to further verify the interaction of the complexes with CT-DNA [33]. Viscosity experiments were conducted on an Ubbelodhe viscometer, immersed in a water bath maintained at 25.0 ± 0.1 °C. Titrations were performed for the complexes (3 μM), and each compound was introduced into the CT-DNA solution (50 μM) present in the viscometer. Data are presented as $(\eta/\eta_0)^{1/3}$ *versus* the ratio of the concentration of the compound to CT-DNA, where η is the viscosity of CT-DNA in the presence of the compound and η_0 is the viscosity of CT-DNA alone. Viscosity values were calculated from the observed flow times of CT-DNA-containing solutions corrected for the flow time in buffer alone (t_0), $\eta = (t - t_0)$ [34].

2.7. *Antioxidation study methods*

The hydroxyl radicals in aqueous media were generated through the Fenton-type reaction [35, 36]. The 3 mL reaction mixtures contained 1.0 mL of 40 μg/mL aqueous safranine, 1 mL of 1.0 mM aqueous EDTA-Fe(II), 1 mL of 3% aqueous H_2O_2, and a series of quantitatively microadding solutions of the tested compound. The sample without the tested compound was used as the control. The reaction mixtures were incubated at 37 °C for 30 min in a water bath. The absorbance was then measured at 520 nm. All the tests were run in triplicate and are expressed as the mean and standard deviation [37]. The scavenging effect for $OH^{\bullet}$ was calculated from the following expression:

$$\text{Scavenging effect}\,\% = (A_{\text{sample}} - A_r)/(A_o - A_r) \times 100\%$$

where A_{sample} is the absorbance of the sample in the presence of the tested compound, A_r is the absorbance of the blank in the absence of the tested compound, and A_o is the absorbance in the absence of the tested compound and EDTA-Fe(II).

3. Results and discussion

The ligand and the complex are very stable in air. They are remarkably soluble in polar aprotic solvents such as DMF and DMSO; slightly soluble in ethanol, methanol, and chloroform; insoluble in water.

3.1. *X-ray structure determination of complexes*

The single-crystal X-ray analysis reveals that the complex crystallizes in monoclinic space group *P2(1)/c* and is a centrosymmetric binuclear neutral entity. The ORTEP structure of Cu(II) complex with atom labeling is shown in figure 1. The structure of the complex consists of two divalent Cu(II) ions, two fully deprotonated ligands and one $CHCl_3$. Both Cu (II) ions are a five-coordinate in a distorted trigonal bipyramidal geometry (figure 1). In the $[Cu_2(L)_2]$•$CHCl_3$ unit, a 10-membered ring is formed by the two Cu(II) centers and the corresponding atoms on the two ligands. Every Cu(II) is N, Ochelated by one ligand and is further N, O coordinated by another ligand. There are two ligands bridged by two Cu(II) ions from the macrocyclic complex. The dinuclear coordination sphere results from fusion of Cu–O and Cu–N bonds. In the ring, the long distance and short distance are 5.937 Å (Cu–Cu) and 3.829 Å (O–O) in the cycle (figure 2). Selected bond lengths and angles of the complex are listed in table 2.

The Cu(II) complex exhibits a different hydrogen-bonding pattern built up from non-classical C–H•••O hydrogen bonds in the crystal structure (figure 3). C–H•••O and C–H•••Cl hydrogen-bonding interactions play important roles in crystal packing in the complex. Selected hydrogen bonds are listed in table 3.

3.2. *IR and electronic spectra*

In free H_2L, a strong band is found at 1637 cm^{-1} together with a weak band at 1286 cm^{-1}. By analogy with the assigned bands, the former can be attributed to $\nu_{(C=N)}$, while the latter can be attributed to $\nu_{(C-O-C)}$. Both bands were shifted to lower frequency by 20–80 cm^{-1} in the spectrum of the complex, which implies coordination of oxygen to the metal. The electronic spectra of the ligands and the metal complex were recorded in DMF solution at room

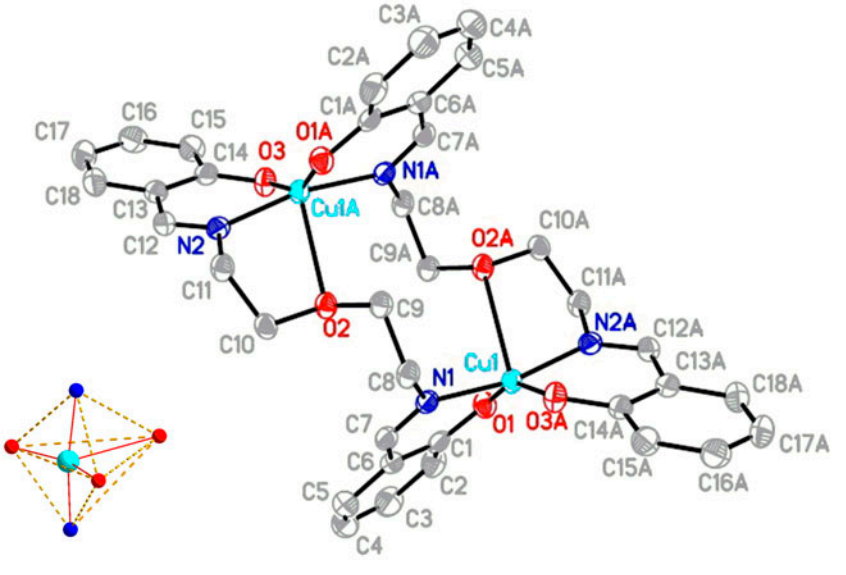

Figure 1. Molecular structure and atom numberings of $[Cu_2(L)_2]$•$CHCl_3$ with hydrogens omitted for clarity.

Table 2. Selected bond distances (Å) and angles (°) for the complex.

Bond distances			
Cu–O(2)	1.9240(15)	Cu–O(1)	1.9266(15)
Cu–N(2)	1.9601(17)	Cu–N(1)	1.9621(18)
Bond angles			
O(2)–Cu–O(1)	153.52(7)	O(2)–Cu–N(2)	92.94(7)
O(1)–Cu–N(2)	90.05(7)	O(2)–Cu–N(1)	90.82(7)
O(1)–Cu–N(1)	91.40(7)	N(2)–Cu–N(1)	168.52(7)
O(3)–Cu–O(1)	121.99(7)	O(3)–Cu–O(2)	83.79(7)
O(3)–Cu–N(1)	72.66(7)	O(3)–Cu–N(1)	96.97(7)
O(3)–Cu–O(2)	83.76(7)		

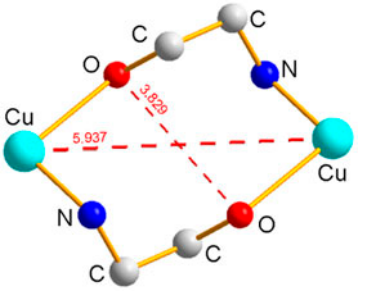

Figure 2. A 10-membered ring of complex.

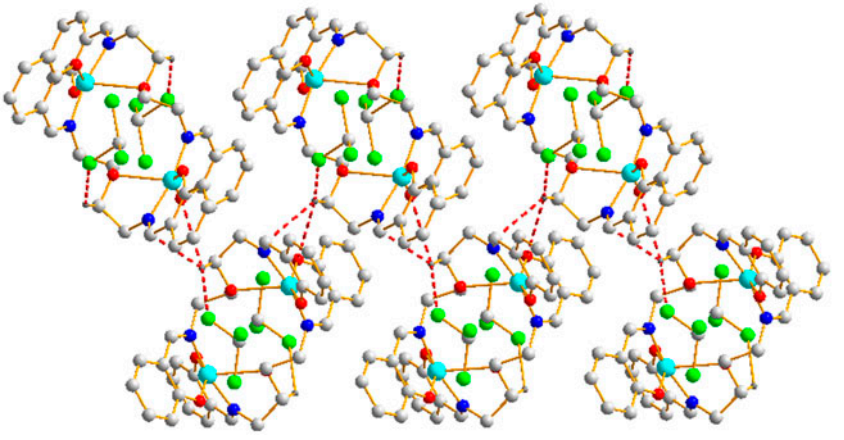

Figure 3. Packing structure of $[Cu_2(L)_2]\cdot CHCl_3$.

temperature. The UV bands of H_2L (275, 311 nm) are marginally shifted in the complex. Two absorption bands are assigned to $\pi \rightarrow \pi^*$ (benzene) and $\pi \rightarrow \pi^*$ (C=N) transitions.

3.3. *DNA-binding mode and affinity*

Electronic absorption spectroscopy is a useful method to study the binding of DNA with metal complexes. The absorption spectra of the ligand and the Cu(II) complex in the

Table 3. Selected hydrogen-bonding distances (Å) and angles (°).

D–H···A	*d*(D–H)	*d*(H···A)	*d*(D···A)	∠(DHA)
C(8)–H(8A)...O(3)#1	0.97	2.42	3.010(3)	118.9
C(11)–H(11B)...O(1)#1	0.97	2.44	2.962(3)	113.2
C(10)–H(10B)...Cl(1)#2	0.97	2.81	3.523(2)	131.0
C(19)–H(19)...O(3)#3	0.98	2.24	3.190(3)	163.5

Note: Symmetry transformations used to generate equivalent atoms: #1 = $-x$, $-y$, $-z+1$; #2 = x, $y-1$, z; #3 = x, $y+1$, z.

absence and presence of CT-DNA (at a constant concentration of compounds) are given in figure 4. H_2L and the Cu(II) complex exhibit intense absorption bands at 395 and 378 nm assigned to π–π^* transition of the C=N, and addition of increasing amounts of CT-DNA results in hypochromism and red shift in the UV–vis spectra of the compounds. In the present case, with the addition of DNA, H_2L, and the Cu(II) complex exhibit hypochromism of 80 and 87% accompanied in the absorption maxima. The spectroscopic changes suggest

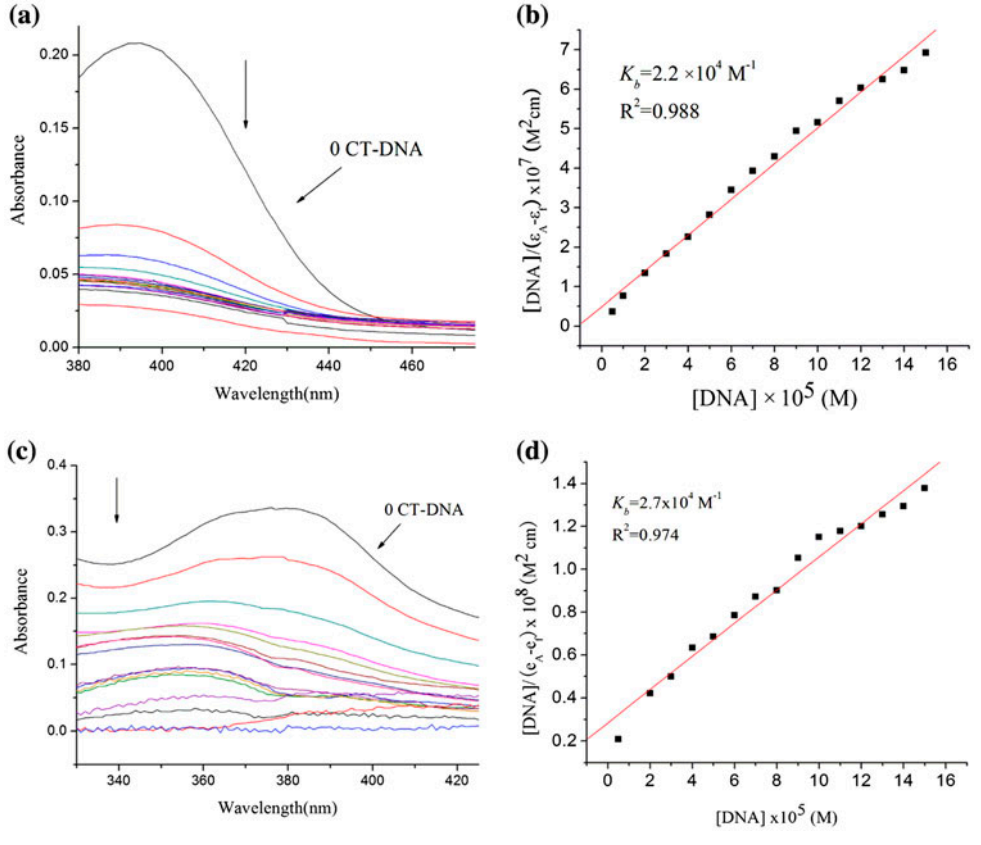

Figure 4. Electronic spectra of H_2L (a), Cu(II) complex (c) in Tris–HCl buffer upon addition of CT-DNA. [Complex] = 3.0×10^{-5} M, [DNA] = 2.5×10^{-5} M. The arrows show the emission intensity changes upon increasing DNA concentration. Plots of $[DNA]/(\varepsilon_a - \varepsilon_f)$ *vs.* [DNA] for the titration of H_2L (b), Cu(II) complex (d) with CT-DNA.

that H_2L and the Cu(II) complex have strong interaction with DNA [38–41]. The K_b values of the H_2L and the Cu(II) complex were 2.2×10^4 M^{-1} (R^2 = 0.988 for 15 points) and 2.7×10^4 M^{-1} (R^2 = 0.974 for 15 points), respectively. Hence, the binding strength of Cu (II) complex is greater than the free ligand. In general, this may be attributed to the Cu(II) complex with the electric effect resulting in relatively close stacking between the Cu(II) complex and the DNA base pairs [41].

Measurement of the ability of a complex to affect the EB fluorescence intensity in the EB-DNA adduct allows determination of the affinity of the complex for DNA, whatever the binding mode may be. No emission was observed either alone or in the presence of CT-DNA in the buffer. A competitive binding of the complex to CT-DNA decreases the emission intensity of EB, and the reduction extent of the emission intensity gives a measure to verify the DNA binding propensity of the complex.

The fluorescence intensity of the EB-DNA system greatly decreases upon gradual addition of both compounds (figure 5). The Stern–Volmer constant K_{SV} was obtained as the slope of the linear plot of I_0/I *versus* compound. From the inset in figure 5, the K_{SV} values are 2.0×10^2 M^{-1} (R^2 = 0.943 for 16 points) and 4.8×10^2 M^{-1} (R^2 = 0.974 for 16 points)

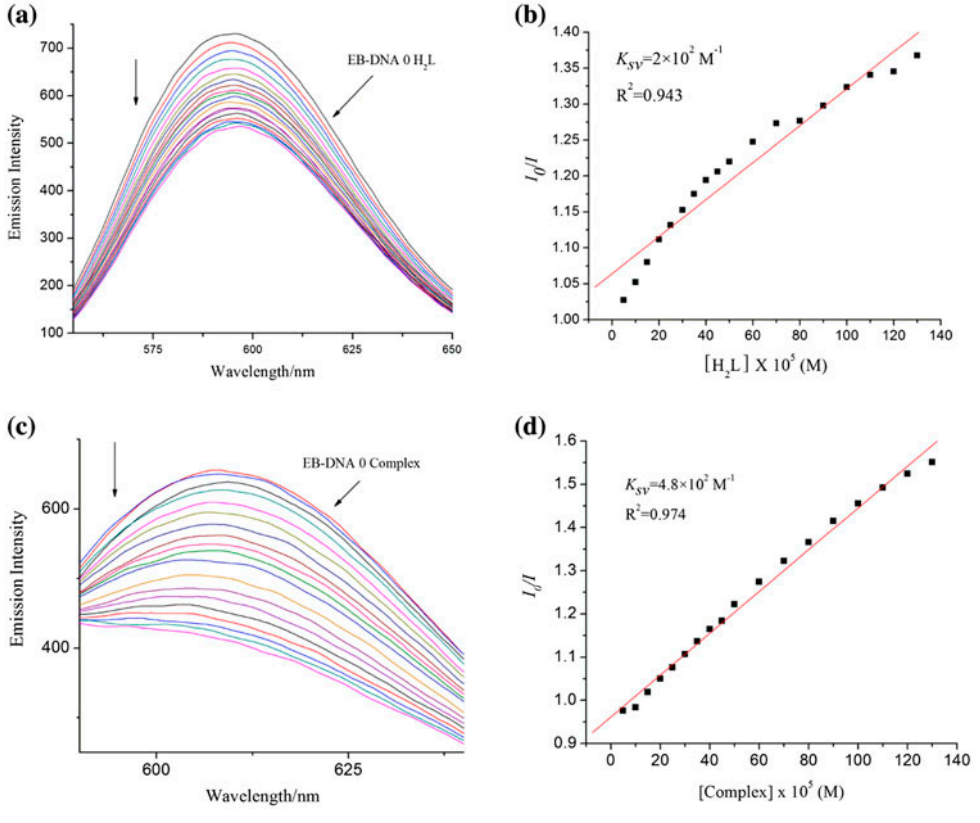

Figure 5. Emission spectra of EB bound to CT-DNA in the presence of free H_2L (a) and Cu(II) complex (c), λ_{ex} = 520 nm. The arrows show the intensity changes upon increasing concentrations of the complexes. Fluorescence quenching curves of EB bound to CT-DNA by free H_2L (b) and Cu(II) complex (d). (Plots of I_0/I *vs.* [complex].)

for H_2L and the complex, respectively. These values show that both the free ligand and complex can compete for DNA-binding sites and so displace EB from the DNA, which is usually characteristic of intercalative interaction of compounds with DNA; the binding strength of the complex is greater than that of the free ligand [42].

Optical photophysical techniques are widely used to study the binding of ligands and their complexes to DNA, but do not give sufficient information to determine a binding model. Therefore, viscosity measurements were carried out to further clarify the interaction of metal complexes and DNA. Hydrodynamic measurements that are sensitive to the length change of DNA (i.e. viscosity and sedimentation) are regarded as the least ambiguous and the most critical tests of a binding model in solution in the absence of crystallographic structural data [43, 44]. For the ligand and the complex, as the amount of compound is increased, the viscosity of DNA increases steadily. The values of $(\eta/\eta_0)^{1/3}$ were plotted against [Complex]/[DNA] (figure 6). In classical intercalation, the DNA helix lengthens as base pairs are separated to accommodate the ligand, leading to increased DNA viscosity, whereas a partial, non-classical ligand intercalation causes a bend (or kink) in the DNA helix, so reducing its effective length and thereby its viscosity [43]. The results shown in figure 6 provide further evidence that both H_2L and the Cu(II) complex intercalate with CT-DNA. The results from the viscosity experiments confirm that these compounds intercalate into DNA base pairs, as also indicated by the spectroscopic studies.

Based on the above results, we found that the affinity for DNA is stronger in Cu(II) complex than with the ligand. We attribute this difference to two possible reasons. (i) By comparison of the molecular structure of the ligand and Cu(II) complexes, we find the greater number of coplanar aromatic rings, which facilitate intercalation to the base pairs of double-helical DNA, may lead to higher affinity for DNA. (ii) The charge transfer of coordinated ligand caused by the coordination of the central atom lead to the decrease in the charge density of the plane conjugate system, which is conducive to insertion [45, 46].

3.4. *Antioxidant activity*

Since H_2L and Cu(II) complex exhibit reasonable DNA-binding affinity, it was considered worthwhile to study other potential aspects, such as antioxidant and antiradical activity. It is

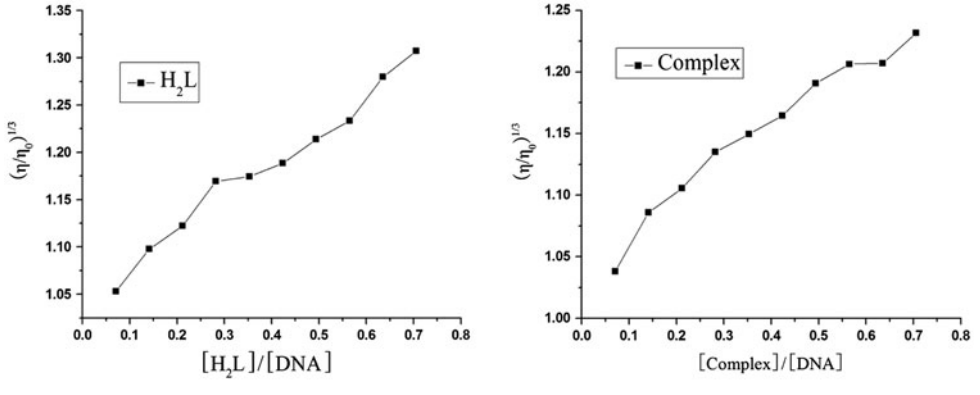

Figure 6. Effect of increasing amounts of the compounds on the relative viscosity at 25.0 ± 0.1 °C.

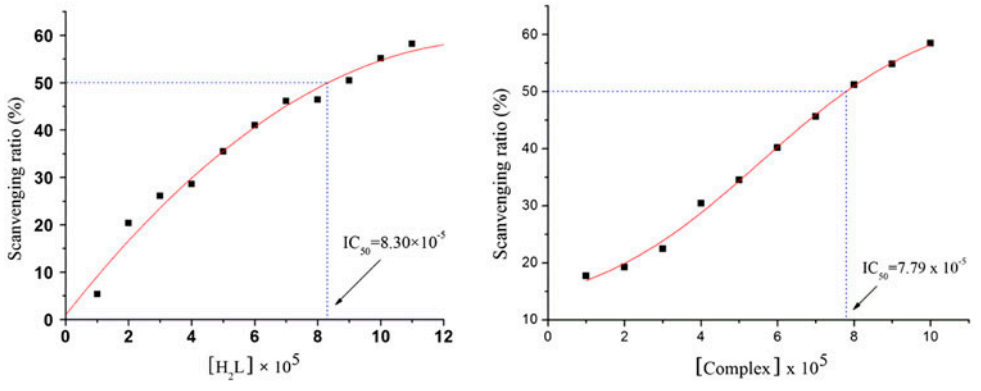

Figure 7. A plot of scavenging percentage (%) *vs.* concentration of the Cu(II) complex on hydroxyl radical.

a well-documented fact that some transition metal complexes display significant antioxidant activity, and therefore, we undertook a systematic investigation on the antioxidant potential of free H_2L and Cu(II) complex against OH• radicals with respect to different concentrations of the test compounds.

Figure 7 depicts the inhibitory effect of H_2L and the complex on OH• radicals. The inhibitory effect of the tested complex on OH• radicals is concentration related, and the suppression ratio increases with increasing the sample concentration of the tested concentration. Mannitol and vitamin C are well-known natural antioxidants, so we also studied the scavenging activity of mannitol and vitamin C against hydroxyl radical using the same model [47]. The 50% inhibitory concentration (IC_{50}) values of mannitol and vitamin C are 9.6×10^{-3} and 8.7×10^{-3} M, respectively. According to the antioxidant experiments, the IC_{50} of the H_2L and Cu(II) complex are 8.30×10^{-5} and 7.79×10^{-5} M (figure 7). We find that when arriving at similar suppression ratio, concentration of the complex and H_2L are far less than that of mannitol and vitamin C. The result showed that the Cu(II) complex exhibits better scavenging activity than H_2L, mannitol, and vitamin C. The lower IC_{50} values observed in antioxidant assays did demonstrate that the Cu(II) complex has a strong potential to be applied as a potential drug to eliminate radicals [36–49].

4. Conclusion

A new unsymmetrical dinuclear Cu complex, $[Cu_2(L)_2]$•$CHCl_3$, has been synthesized and characterized by single-crystal X-ray diffraction based on the Schiff base bis(*N*-salicylidene)-3-oxapentane-1,5-diamine (H_2L). The binding modes of ligand and Cu(II) complex with CT-DNA have been studied. The photophysical and viscosity measurements indicate that the compounds interact with CT-DNA through intercalative binding and their affinity to DNA follows the order complex > ligand, which can be attributed to the difference in steric hindrance and electron density caused by coordination. In addition, ligand and Cu(II) complex also reveal excellent antioxidant properties, with complex more effective than ligand. These compounds have potential applications for the development of nucleic acid molecular probes and new therapeutic reagents for diseases on the molecular level and warrant further *in vivo* experiments and pharmacological assays.

Supplementary material

Crystallographic data (excluding structure factors) for the structure in this article have been deposited with the Cambridge Crystallographic Data Center as supplementary publication CCDC 835709. Copies of the data can be obtained free of charge on application to the CCDC, 12 Union Road, Cambridge CB2 1EZ, UK.

Funding

The present research was supported by the National Natural Science Foundation of China [grant number 21367017]; the Fundamental Research Funds for the Gansu Province Universities [grant number 212086]; Natural Science Foundation of Gansu Province [grant number 1212RJZA037]; "Qing Lan" Talent Engineering Funds for Lanzhou Jiaotong University.

References

[1] A.A.A. Abu-Hussen, Y.K. Al-Majedy, H.H. Ibrahim, A.A. Al-Tamimi. *J. Coord. Chem.*, **59**, 157 (2006).
[2] M.S. Karthikeyan, D.J. Prasad, B. Poojary, K.S. Bhat, B.S. Holla, N.S. Kumari. *Bioorg. Med. Chem.*, **14**, 7482 (2006).
[3] K. Singh, M.S. Barwa, P. Tyagi. *Eur. J. Med. Chem.*, **41**, 147 (2006).
[4] P. Panneerselvam, R.B. Nair, G. Vijayalakshmi, E.H. Subramanian, S.K. Sridhar. *Eur. J. Med. Chem.*, **40**, 225 (2005).
[5] S.K. Sridhar, M. Saravanan, A. Ramesh. *Eur. J. Med. Chem.*, **36**, 615 (2001).
[6] R. Mladenova, M. Ignatova, N. Manolova, T. Petrova, I. Rashkov. *Eur. Polym. J.*, **38**, 989 (2002).
[7] H. Yu, S.L. Le, X.H. Zeng, J.Y. Zhang, J.L. Xie. *Inorg. Chem. Commun.*, **39**, 135 (2014).
[8] W.K. Dong, L. Li, Y.X. Sun, J.F. Tong, J.C. Wu. *Transition Met. Chem.*, **35**, 787 (2010).
[9] Q. Liu, Y.S. Yang, W.D. Hao, Z.H. Xu, L.H. Zhu. *IERI Procedia*, **5**, 178 (2013).
[10] S. Thalamuthu, B. Annaraj, M.A. Neelakantan. *Spectrochim. Acta, Part A*, **118**, 120 (2014).
[11] X.L. Wang, M. Jiang, Y.T. Li, Z.Y. Wu, C.W. Yan. *J. Coord. Chem.*, **66**, 1985 (2013).
[12] Y. Mei, J.J. Zhou, H. Zhou, Z.Q. Pan. *J. Coord. Chem.*, **65**, 643 (2012).
[13] L.M. Wilhelmsson, F. Westerlund, P. Lincoln, B. Nordén. *J. Am. Chem. Soc.*, **124**, 12092 (2002).
[14] F. Wang, J.L. Wang, Y.M. Zhai, G.P. Li, D. Li, S.J. Dong. *J. Control. Release*, **132**, 65 (2008).
[15] W. Hu, S.W. Deng, J.Y. Huang, Y.M. Lu, X.Y. Le, W.X. Zheng. *J. Inorg. Biochem.*, **127**, 90 (2013).
[16] H.L. Wu, K.T. Wang, F. Jia, B. Liu, F. Kou, J.K. Yuan, J. Kong. *J. Coord. Chem.*, **63**, 4113 (2010).
[17] N. Shahabadi, S. Kashanian, F. Darabi. *Eur. J. Med. Chem.*, **45**, 4239 (2010).
[18] V. Uma, V.G. Vaidyanathan, B.U. Nair. *Bull. Chem. Soc. Jpn.*, **78**, 845 (2005).
[19] K.E. Erkkila, D.T. Odom, J.K. Barton. *Chem. Rev.*, **99**, 2777 (1999).
[20] V. Uma, M. Kanthimathi, T. Weyhermuller, B.U. Nair. *J. Inorg. Biochem.*, **99**, 2299 (2005).
[21] B.M. Zeglis, V.C. Pierre, J.K. Barton. *Chem. Commun.*, **44**, 4565 (2007).
[22] H.L. Wu, X.C. Huang, J.K. Yuan, F. Kou, F. Jia, B. Liu, K.T. Wang. *Eur. J. Med. Chem.*, **45**, 5324 (2010).
[23] H.L. Wu, F. Jia, F. Kou, B. Liu, J.K. Yuan, Y. Bai. *J. Coord. Chem.*, **64**, 3454 (2011).
[24] H.L. Wu, J.K. Yuan, Y. Bai, F. Jia, B. Liu, F. Kou, J. Kong. *Transition Met. Chem.*, **36**, 819 (2011).
[25] G.L. Pan, Y.C. Bai, H. Wang, J. Kong, F.R. Shi, Y.H. Zhang, X.L. Wang, H.L. Wu. *Z. Naturforsch. B*, **68b**, 257 (2013).
[26] Bruker. *APEX2 and SAINT*, Bruker AXS Inc., Madison, WI (2007).
[27] G.M. Sheldrick. *Acta Cryst. A*, **64**, 112 (2008).
[28] R.K. Bindiya, S. Pramodini, R.K. Bhubon, R.K. Hemakumar, T. Swub, W. Radhapiyari, Ch. Brajakishore. *J. Coord. Chem.*, **67**, 891 (2014).
[29] Z.X. Su, Y.Q. Wan, H.L. Wu. *Synth. React. Inorg. Met. Org. Chem.*, **35**, 553 (2005).
[30] S. Yellappa, J. Seetharamappa, L.M. Rogers, R. Chitta, R.P. Singhal, F.D. D'Souza. *Bioconjugate Chem.*, **17**, 1418 (2006).
[31] S.A. Patil, S.N. Unki, A.D. Kulkarni, V.H. Naik, U. Kamble, P.S. Badami. *J. Coord. Chem.*, **64**, 323 (2011).
[32] N. Raman, A. Sakthivel, R. Jeyamurugan. *J. Coord. Chem.*, **63**, 1080 (2010).
[33] J. Lu, J.L. Li, Q. Sun, L. Jiang, B.W. Wang, W. Gu, X. Liu, J.L. Tian, S.P. Yan. *J. Coord. Chem.*, **67**, 300 (2014).
[34] C.P. Tan, J. Liu, L.M. Chen, S. Shi, L.N. Ji. *J. Inorg. Biochem.*, **102**, 1644 (2008).
[35] Z.Y. Guo, R.E. Xing, S. Liu, H.H. Yu, P.B. Wang, C.P. Li, P.C. Li. *Bioorg. Med. Chem. Lett.*, **15**, 4600 (2005).
[36] Z.C. Liu, B.D. Wang, Z.Y. Yang, Y. Li, D.D. Qin, T.R. Li. *Eur. J. Med. Chem.*, **44**, 4477 (2009).

[37] H.L. Wu, Y. Bai, J.K. Yuan, H. Wang, G.L. Pan, X.Y. Fan, J. Kong. *J. Coord. Chem.*, **65**, 2839 (2012).
[38] A.M. Pyle, J.P. Rehmann, R. Meshoyrer, C.V. Kumar, N.J. Turro, J.K. Barton. *J. Am. Chem. Soc.*, **111**, 3051 (1989).
[39] Q.L. Zhang, J.H. Liu, J.Z. Liu, P.X. Zhang, X.Z. Ren, Y. Liu, Y. Huang, L.N. Ji. *J. Inorg. Biochem.*, **98**, 1405 (2004).
[40] R. Indumathy, T. Weyhermüller, B.U. Nair. *Dalton Trans.*, **39**, 2087 (2010).
[41] C.Y. Gao, X.F. Ma, J. Lu, Z.G. Wang, J.L. Tian, S.P. Yan. *J. Coord. Chem.*, **64**, 2157 (2011).
[42] M. Shakir, M. Azam, M.-F. Ullah, S.-M. Hadi. *J. Photochem. Photobiol. B*, **104**, 449 (2011).
[43] G.J. Chen, X. Qiao, P.Q. Qiao, G.J. Xu, J.Y. Xu, J.L. Tian, W. Gu, X. Liu, S.P. Yan. *J. Inorg. Biochem.*, **105**, 119 (2011).
[44] T.R. Li, Z.Y. Yang, B.D. Wang, D.D. Qin. *Eur. J. Med. Chem.*, **43**, 1688 (2008).
[45] S. Yellappa, J. Seetharamappa, L.M. Rogers, R. Chitta, R.P. Singhal, F. D'Souza. *Bioconjugate Chem.*, **17**, 1418 (2006).
[46] M. Shakir, M. Azam, M.F. Ullah, S.M. Hadi. *J. Photochem. Photobiol. B*, **104**, 449 (2011).
[47] P.X. Xi, Z.H. Xu, X.H. Liu, F.J. Chen, Z.Z. Zeng, X.W. Zhang, Y. Liu. *J. Fluoresc.*, **19**, 63 (2007).
[48] M.N. Patel, D.S. Gandhi, P.A. Parmar. *Inorg. Chem. Commun.*, **13**, 618 (2010).
[49] J.E. Weder, C.T. Dillon, T.W. Hambley, B.J. Kennedy, P.A. Lay, J. Biffin, H.L. Regtop, N.M. Davies. *Coord. Chem. Rev.*, **232**, 95 (2002).